Patricio F. Mendez
Professor
Mem. ASME
Chemical and Materials Engineering,
University of Alberta,
Donadeo ICE 12-332 9211 116 St,
Edmonton, AB T6G 2V4
e-mail: pmendez@ualberta.ca

Yi Lu
Chemical and Materials Engineering,
University of Alberta,
Edmonton, AB T6G 2R3, Canada
e-mail: ylu13@ualberta.ca

Ying Wang[1]
Chemical and Materials Engineering,
University of Alberta,
Edmonton, AB T6G 2R3, Canada
e-mail: wang18@ualberta.ca

Scaling Analysis of a Moving Point Heat Source in Steady-State on a Semi-Infinite Solid

This paper presents a systematic scaling analysis of the point heat source in steady-state on a semi-infinite solid. It is shown that all characteristic values related to an isotherm can be reduced to a dimensionless expression dependent only on the Rykalin number (Ry). The maximum width of an isotherm and its location are determined for the first time in explicit form for the whole range of Ry, with an error below 2% from the exact solution. The methodology employed involves normalization, dimensional analysis, asymptotic analysis, and blending techniques. The expressions developed can be calculated using a handheld calculator or a basic spreadsheet to estimate, for example, the width of a weld or the size of zone affected by the heat source in a number of processes. These expressions are also useful to verify numerical models. [DOI: 10.1115/1.4039353]

1 Introduction

The problem of moving heat sources is central to a wide range of fields including welding [1–3], heat treatment [4–6], tribology [7,8], grinding [9,10], machining [11,12], wheel and track contact [13,14], and many more. This problem has been approached analytically [1,2,3,15] and numerically by many researchers (e.g., Refs. [16] and [17]), and there is a vast wealth of known expressions related to moving heat sources [18]; however, the current knowledge of moving heat sources is often difficult to apply in engineering practice.

Numerical solutions are often difficult to implement for practitioners without specialized software or not versed in computational modeling. Also, numerical solutions published are valid for the particular values of parameters considered in each publication, but difficult to generalize to practical cases with different parameters.

Empirical models typically have the advantage of simplicity, but also a limited amount of generality. Their range of application is typically limited to the particular material system and conditions under which they were developed. The theoretical foundation of empirical models is seldom strong enough to extrapolate them beyond the tested conditions; often, their range of validity is not stated explicitly, leaving practitioners at risk of unknowingly using the models beyond their predictive abilities.

Analytical solutions have the advantage of relative simplicity and strong theoretical foundation, but also have limitations in practice. Sometimes they often involve series summations [15] or improper integrals that require careful computational implementation, especially for the case of distributed heat sources [19–22]. Also, analytical solutions typically have inconvenient expressions for addressing practical questions. Analytical solutions typically have the form of temperature as a function of time and space coordinates. When using Eulerian coordinates, typically a steady-state is considered, obtaining $T = T(x, y, z)$, with a typical coordinate system represented in Fig. 1.

Practical questions are not easily answered by analytical expressions; for example, the question of "what is the weld width?" is difficult to answer, even as a rough approximation, using the simplest of models. The answer to this question is given by the maximum width of isotherm corresponding to the melting temperature. In a steady-state process, this would correspond to solving for y the implicit equation $T(x, y, z) = T_m$, and then finding the maximum value of y for any x. This maximum is typically obtained using numerical methods. Similar questions are: "what is the cooling rate at a point after the heat source passed over it?" (crucial for material properties after welding, heat treatment and material removal), "what is the heating rate as the heat source approaches?" (important to assess austenization temperature in laser heat treating of steels), "what is the maximum temperature?" (important in almost all applications and materials systems). In all these cases, the answer involves solving an implicit equation. An additional challenge for practitioners is that moving heat sources involve a large number of parameters, making an intuitive grasp of the problem difficult to obtain [23,24]. One promising approach using the concept of thermal resistance is presented in Ref. [25].

Textbooks often omit a treatment of moving heat sources (e.g., Ref. [26]) or introduce the foundations for mathematical or numerical analysis, often based on Green's functions (e.g., Ref. [27]), but do not present expressions amenable to use by practitioners. Similarly, handbooks do not present a general, well-structured treatment of moving heat sources, describing the mathematical foundations and some particular expressions (often

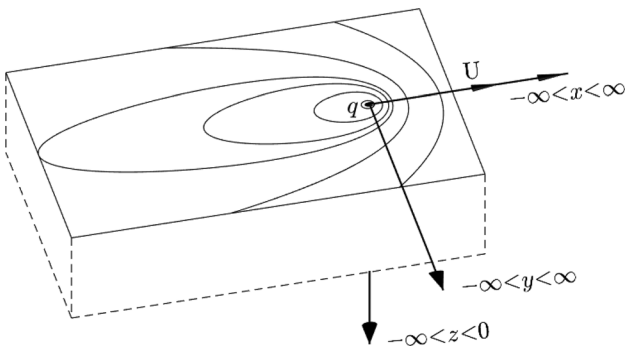

Fig. 1 Point heat source moving with constant velocity on a semi-infinite solid

[1]Corresponding author.

Contributed by the Heat Transfer Division of ASME for publication in the Journal of Heat Transfer. Manuscript received December 1, 2017; final manuscript received February 1, 2018; published online April 11, 2018. Assoc. Editor: Alan McGaughey.

empirical, e.g., Refs. [18] and [28]). To the best of our knowledge, neither textbooks nor handbooks present general practical expressions for the maximum width of an isotherm and other related quantities. One consequence of the challenges described previously is that practitioners typically learn heuristics that are material-specific or process-specific and there is little transfer of knowledge between specialists. Steel welding experts can seldom extend their expertise to aluminum welding, and welding specialists seldom inform or are informed by grinding or machining experts, despite that the problems each specialist tackles responds to very similar heat transfer phenomena.

This paper is the first step of a broader research program aimed at identifying moving heat source features of interest to practitioners and presenting practical and accurate predictive expressions useful to them. The overall research program is based on the understanding that many important aspects of complex problems such as welding can be treated using a minimal representation that captures only the dominant physics, with the secondary physics included as correction factors. This approach is often used in all engineering disciplines at an intuitive level, and a formal implementation is described in Refs. [23], [24], and [29].

Sections 2 and 3 introduce selected characteristic values of interest to practitioners, then dimensional analysis is applied to determine that each dimensionless characteristic value depends only on one dimensionless group that determines two asymptotic regimes. A closed-form expression of the characteristic values in each Regime is presented, and blending functions are used to estimate the characteristic values at the intermediate regime with high accuracy and practical simplicity. The blending functions are also the basis of correction factors of the form typically used in engineering applications.

2 Governing Equation

The model of heat source analyzed is the one typically attributed to Rosenthal [1,2] or Rykalin [3], but that has been solved before in 1904 by Wilson [30] and in 1923 by Roberts [31] (for the case of mass transfer). The model is illustrated in Fig. 1 and consists of a point heat source of intensity q moving in steady-state along a straight line (x-axis) with constant velocity U on the flat surface of a semi-infinite solid with constant thermophysical properties. This model must be used with an understanding of the limitations. For the case in which there is fusion of the base material, such as in welding, this model does not account for the effects of convective heat transfer in the molten metal, the effect of latent heat of melting, or the phase transformations. For the particular case of welding applications, this model is reasonably accurate for temperatures significantly below the melting temperature. Size and shape of the weld bead are defined by the melting isotherm, and only their order of magnitude is captured [32]. Despite its limitations, the point heat source model is invaluable for rough estimates and trends. The governing equation for this point heat source problem is

$$\frac{\partial^2 T}{\partial x^2}+\frac{\partial^2 T}{\partial y^2}+\frac{\partial^2 T}{\partial z^2}+\frac{U}{\alpha}\frac{\partial T}{\partial x}=0 \tag{1}$$

where x, y, and z are the coordinates illustrated in the schematic of Fig. 1 and constitute the independent variables. This mathematical formulation involves an Eulerian coordinate frame, in which the heat source is the stationary origin and the substrate moves in the $-x$ direction, instead of a heat source moving in the $+x$ direction on a stationary substrate. The temperature, $T=T(x, y, z)$, is the dependent variable and also depends on the problem parameters. U is the magnitude of the velocity of the heat source relative to the substrate, and α is the thermal diffusivity of the substrate. Equation (1) is defined in the domain $z \geq 0$ and $r \geq \varepsilon$, where ε is an arbitrary small number and the radial coordinate, r, is defined in relation to the independent variables as

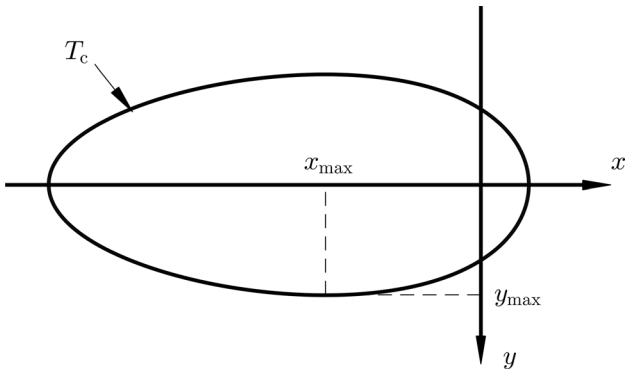

Fig. 2 Characteristic values y_{max} and x_{max} for a point heat source moving with constant velocity on a semi-infinite solid

$$r=\sqrt{x^2+y^2+z^2} \tag{2}$$

The boundary conditions for Eq. (1) are

$$\frac{\partial T}{\partial z}=0 \quad \text{for } z=0,\ r\geq\varepsilon \tag{3}$$

$$\frac{\partial T}{\partial r}=\frac{q}{2\pi k\varepsilon^2} \quad \text{for } r=\varepsilon,\ z\geq 0 \tag{4}$$

$$T=T_0 \quad \text{for } r\to\infty,\ z\geq 0 \tag{5}$$

where q is the thermal power from the heat source absorbed by the solid, k is the thermal conductivity of the substrate, and T_0 is the temperature of the substrate far from the heat source. For problems such as welding, the power q is estimated based on the nominal power of the heat source and a thermal efficiency. The solution to Eq. (1) with boundary conditions from Eqs. (3)–(5) is

$$T(x,y,z)=T_0+\frac{q}{2\pi kr}\exp\left[-\frac{U}{2\alpha}(r+x)\right] \tag{6}$$

Equation (6) provides the value of temperature for each point in the domain, with a singularity at $r=0$, which is the location of the heat source. The singularity is not observed in practical systems, and other models have been proposed for analyzing the temperature field near the heat source (e.g., Gaussian distribution heat sources [19]). The solution also has symmetry of revolution around the x-axis, and the cross section of all isotherms on a y-z plane is semicircular.

In practical applications, questions typically focus on characteristic values of the solution, for example maximum width of an isotherm or maximum temperature at a given point. The concept of characteristic values is discussed in detail in Ref. [33]. In the model studied here, for reasons of length, the asymptotic analysis is limited to the maximum width of the isotherm, $T(x, y, z)=T_c$, and its location (y_{max} and x_{max} corresponding to the plane $z=0$) illustrated in Fig. 2. The semicircular nature of isotherms on the y-z plane implies that the penetration under the surface z_{max} is the same as the width y_{max} and both maxima are located at the same coordinate $x=x_{max}$. The asymptotic analysis of other characteristic values is the subject of current research to be published separately.

3 Scaling Analysis Methodology

The methodology of analysis is described in Ref. [29], and consists in finding a minimal representation of the problem, which is an asymptotic solution, and then developing a correction factor that relates the asymptotic solution to intermediate cases. The use of correction factors is common in engineering and allows for the

simultaneous benefits of practical expressions and accurate predictions within the range of validity of the correction factors.

3.1 Normalization. The first step toward a minimal representation is normalization, in which the original equations are reduced to their dimensionless counterparts. In this case, Eq. (6) can be rewritten in normalized form as

$$T^* = \frac{1}{r^*}\exp(-r^* - x^*) \tag{7}$$

where

$$T^* = \frac{4\pi k\alpha(T - T_0)}{qU} \tag{8}$$

$$x^* = \frac{Ux}{2\alpha} \tag{9}$$

$$y^* = \frac{Uy}{2\alpha} \tag{10}$$

$$z^* = \frac{Uz}{2\alpha} \tag{11}$$

$$r^* = \frac{Ur}{2\alpha} \tag{12}$$

In Eqs. (8)–(12), the * superscript indicates a dimensionless quantity, consistent with Refs. [33] and [34] and other modern literature. Equation (7) involves four dimensionless groups: the three independent variables x^*, y^*, and z^* (r^* is not independent) and the dependent variable $T^*(x^*, y^*, z^*)$. There is no other dimensionless group associated with the parameters.

The number of dimensionless groups is consistent with the number expected from applying dimensional analysis theory [35]. Dimensional analysis theory states that the number of dimensionless groups in a problem is given by the number of magnitudes with dimension minus the number of independent units involved, and minus one when the temperature is not measured in absolute terms [36]. Equation (6) involves nine magnitudes with units: the three independent variables x, y, and z, the dependent variable $T(x, y, z)$, and the five problem parameters T_0, q, k, U, and α. There are four independent units for the magnitude with dimension (m, kg, s, °C) and the number of dimensionless groups is $9-4-1=4$. Since there are four variables (three independent and one dependent), the dimensionless expression of each variable can become a dimensionless group, leaving no room for an additional dimensionless group unrelated to any variable.

The dimensional analysis result is important as it confirms that there is no variable-free dimensionless group. This is in contrast to the normalization proposed by Christensen et al. [32], where five dimensionless groups were proposed resulting in a nonindependent set that unnecessarily complicates the analysis and is misleading. The five dimensionless groups proposed in Ref. [32] are λ (x^* here), ψ (y^* here), ζ (z^* here), θ, and n. The ratio θ/n is equivalent to T^* here. In Christensen's analysis, θ and n appear separate through the consideration of an arbitrary "chosen reference level" (T_c in Ref. [32] but with a different meaning than the symbol T_c used here) in addition of the temperature field $T(x, y, z)$. The "chosen reference level" is often associated with the melting temperature of the base material but has no physical meaning in the context of the original governing equation, which does not consider melting or any other phase transformation. The parameter n appears to be a dimensionless group related only to problem parameters despite that such a parameter does not exist under rigorous analysis. Christensen's notation, despite the shortcoming of having a redundant dimensionless group, has been used in important follow-up work such as Refs. [19], [37], and [38].

The dimensionless form of the characteristic values associated with the isotherm $T = T_c$ depend only on one dimensionless group. It is important to keep in mind that T_c is a value that defines an isotherm by constraining the field $T(x, y, z)$ to a constant value. In contrast to Christensen's analysis, T_c is a constraint of the temperature field rather than an additional parameter; isotherms in Christensen analysis would require an additional constraint. Considering the maximum width of an isotherm in dimensionless form ($y^*_{\max}$), Eq. (7) involves four degrees-of-freedom (DOFs), related to the four independent dimensionless groups (x^*, y^*, z^*, T^*). One constraint is Eq. (7), leaving only three degrees-of-freedom between dimensionless groups. The definition of $y^*_{\max}$ involves two more constraints: $z^* = 0$, and $y^*_{\max} = \max(y^*)$, leaving only one degree-of-freedom. This degree-of-freedom can be assigned to any of an infinite array of suitable dimensionless groups. The Rykalin number (Ry) proposed by Fuerschbach and Eisler [39] will be used to capture the remaining degree-of-freedom

$$\mathrm{Ry} = \frac{qU}{4\pi k\alpha(T_c - T_0)} \tag{13}$$

where the factor of $1/4\pi$ is included to simplify the final expressions detailed below.

The Rykalin number can be interpreted as a Peclet number ($\mathrm{Pe} = U\mathcal{L}/\alpha$) where the characteristic length $\mathcal{L}$ is related to the gradient induced by the heat source: $\mathcal{L} = q/[4\pi k(T_c - T_0)]$. The Peclet number relates the effect of advection relative to conduction, and therefore, a high Ry value can be interpreted as a "fast heat source" where advection dominates over conduction, and a low Ry value can be interpreted as a "slow heat source" with heat transfer dominated by conduction.

Based on dimensional analysis and the choice of Ry to capture the one degree-of-freedom of this problem, all dimensionless characteristic values associated with an isotherm can be captured with functions depending only on Ry, thus $y^*_{\max} = y^*_{\max}(\mathrm{Ry})$ and $x^*_{\max} = x^*_{\max}(\mathrm{Ry})$.

The value of Ry can range between zero and infinity, defining two asymptotic regimes for the characteristic values: Regime I, corresponding to large values of Ry (fast), and Regime II, corresponding to small values of Ry (slow). These asymptotic regimes yield simple expressions for the characteristic values, usually in the form of power laws.

3.2 Blending of Asymptotic Solutions. The simple expressions obtained for each asymptotic regime are less accurate for intermediate values ($\mathrm{Ry} = \mathrm{O}(1)$). For these intermediate values, simple and accurate expressions can be obtained using the blending functions proposed by Churchill and Usagi [40].

For the dimensionless maximum isotherm width $y^*_{\max}(\mathrm{Ry})$, the associated asymptotic expression for Regime I is $\hat{y}^*_{\max_\mathrm{I}}(\mathrm{Ry})$, and for Regime II is $\hat{y}^*_{\max_\mathrm{II}}(\mathrm{Ry})$. In this notation, the symbol $\hat{}$ indicates that the magnitude is an asymptotic approximation. The blending functions proposed for the isotherm width have the following expression:

$$y^*_{\max}(\mathrm{Ry}) \approx \hat{y}^{*+}_{\max}(\mathrm{Ry}) = [\hat{y}^*_{\max_\mathrm{I}}(\mathrm{Ry})^n + \hat{y}^*_{\max_\mathrm{II}}(\mathrm{Ry})^n]^{1/n} \tag{14}$$

where n is the blending parameter and the $^+$ superscript indicates improvement over the asymptotic approximations. A very important aspect of Eq. (14) is that the expression gives the exact asymptotic behavior for both regimes for all finite values of n. The error is not zero for intermediate values of Ry and is defined here as

$$\mathrm{error} = \ln\frac{\hat{y}^{*+}_{\max}}{y^*_{\max}} \tag{15}$$

This definition of error is consistent with Refs. [33], [41], and [42], and it offers the advantage of yielding comparable

magnitudes for large errors in excess or defect, and being convenient for power-law expressions. For small errors, this definition is equivalent to the standard definition of relative error.

The value of n is determined with a numerical optimization procedure, and it can be positive or negative, with absolute values typically of the order of magnitude of 1. The parameter n needs to be determined only once for each blending function.

3.3 Development of Correction Factors. Equation (14) can also be used to create correction factors that extend the usefulness of the asymptotic expressions. In this work, the correction factors are accurate for intermediate values and beyond, all the way to the opposite asymptotic regimes. The correction factors $f_{y_{\max_I}}(\mathrm{Ry})$ and $f_{y_{\max_{II}}}(\mathrm{Ry})$, associated with the characteristic value $y_{\max}$, are based on the asymptotic expressions and have the following expressions:

$$y_{\max} \approx \hat{y}^{+}_{\max} = \hat{y}_{\max_I}\left\{1+\left[\frac{\hat{y}^{*}_{\max_{II}}(\mathrm{Ry})}{\hat{y}^{*}_{\max_I}(\mathrm{Ry})}\right]^{n}\right\}^{1/n} = \hat{y}_{\max_I} f_{y_{\max_I}}(\mathrm{Ry}) \quad \text{for Regime I (fast)} \tag{16}$$

$$y_{\max} \approx \hat{y}^{+}_{\max} = \hat{y}_{\max_{II}}\left\{1+\left[\frac{\hat{y}^{*}_{\max_{II}}(\mathrm{Ry})}{\hat{y}^{*}_{\max_I}(\mathrm{Ry})}\right]^{-n}\right\}^{1/n} = \hat{y}_{\max_{II}} f_{y_{\max_{II}}}(\mathrm{Ry}) \quad \text{for Regime II (slow)} \tag{17}$$

Equations (16) and (17) are exactly equivalent and they are the same approximation to the exact solution, but based on different starting asymptotic expressions. As the Rykalin number approaches infinity (Regime I), $f_{y_{\max_I}}(\mathrm{Ry})$ tends to 1 and for Ry approaching 0, $f_{y_{\max_{II}}}(\mathrm{Ry})$ tends to 1. The value of n for Eqs. (16) and (17) are the same as for Eq. (14).

Because $\hat{y}^{*}_{\max_I}(\mathrm{Ry})$ and $\hat{y}^{*}_{\max_{II}}(\mathrm{Ry})$ have simple expressions, typically of the form of power laws, the correction factors also have closed-form expressions that are simple to calculate in a handheld calculator or a spreadsheet. The simplicity of the expressions, their generality, and their accuracy make the correction factors powerful tools for practical calculations.

4 Scaling Analysis of Maximum Isotherm Width $y_{\max}$

The magnitude $y_{\max}$ is the maximum width of the isotherm $T(x, y, z) = T_c$ corresponding to the plane $z = 0$, as illustrated in Fig. 2. The dimensionless width $y^{*}_{\max}(\mathrm{Ry})$ requires a numerical optimization to find the maximum for each Rykalin number considered, and its dependence on Ry is illustrated in Fig. 3. The asymptotic behavior at high and low Ry is straight lines in log–log scale, indicating a power-law behavior.

Asymptotic analysis of Eq. (7), detailed in the Appendix, yields the following power laws:

$$\hat{y}^{*}_{\max_I}(\mathrm{Ry}) = \sqrt{\frac{2\mathrm{Ry}}{\mathrm{e}}} \quad \text{for Regime I (fast)} \tag{18}$$

$$\hat{y}^{*}_{\max_{II}}(\mathrm{Ry}) = \mathrm{Ry} \quad \text{for Regime II (slow)} \tag{19}$$

The blending expression for $\hat{y}^{+}_{\max}(\mathrm{Ry})$ is given by Eq. (14). Replacing the expressions for $\hat{y}^{*}_{\max_I}(\mathrm{Ry})$ and $\hat{y}^{*}_{\max_{II}}(\mathrm{Ry})$ into Eqs. (16) and (17), the following expressions for the correction factors are obtained:

$$f_{y_{\max_{I,II}}}(\mathrm{Ry}) = \left[1+\left(\sqrt{\frac{\mathrm{eRy}}{2}}\right)^{\pm n}\right]^{1/n} \tag{20}$$

where the exponent $+n$ corresponds to Regime I, and $-n$ corresponds to Regime II. The value of n was determined using a minimax approach with nested optimizations. In the first optimization, a value of n was assumed, and the error was calculated using Eq. (15) for a relevant range of values of Ry. Figure 4 illustrates the error variation as a function of Ry for three values of n. This figure also displays two important features: The error tends to zero for both high and low Ry, as expected, and the maximum absolute value of error (error ceiling for a given n) occurs simultaneously at $\mathrm{Ry} = 0.0632$ and $\mathrm{Ry} = 1.5215$ for the value of $n = -1.7312$. The reason for this simultaneous maxima is illustrated in Fig. 4. For values of n above the optimal, the ceiling of error is given by the peak on the right; for values of n below the optimal, the ceiling of error is given by the valley on the left, and at the optimal value, both peaks coincide with the same ceiling of error.

In the second nested optimization, different values of n are explored to find the value of n which yields the minimum maximum (minimax) absolute value of error, or minimum error ceiling. Figure 5 represents the variation in maximum absolute value of error as a function of n. It is seen that at the optimal value of n ($n = -1.7312$), the minimax error is 0.7236%. The sharp minimum at that point is the consequence of tracking different local extremes above or below the optimum value of n.

The correction factors for both regimes (Eq. (20)) are illustrated in Fig. 6. These correction factors based on blending have an error smaller than 0.7236% compared with the exact solution for any

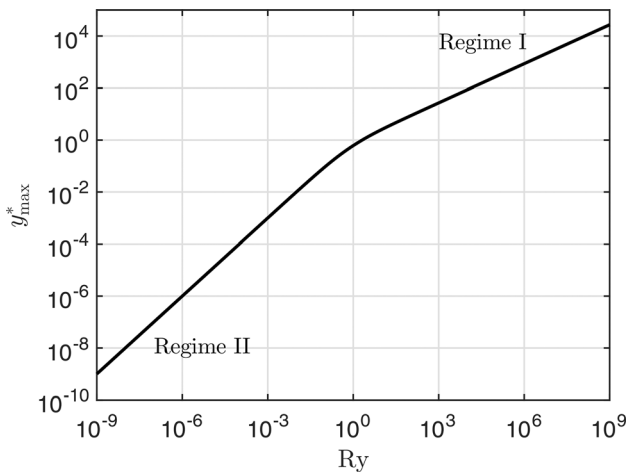

Fig. 3 Dimensionless isotherm width $y^{*}_{\max}$ as a function of Ry

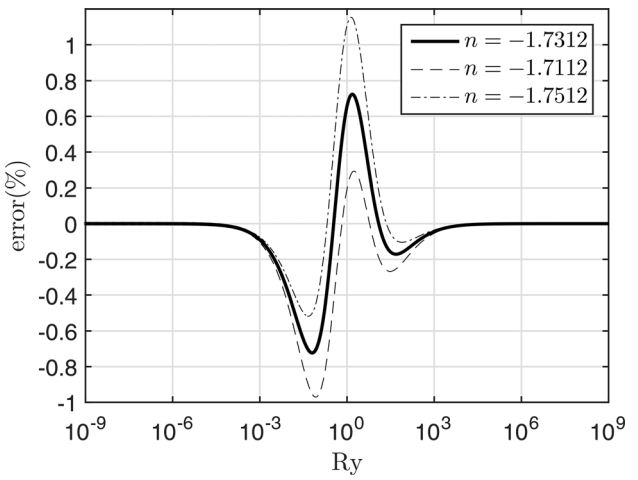

Fig. 4 Blending error for isotherm width $y_{\max}$ as a function of Ry for exponents n at or near the optimal value

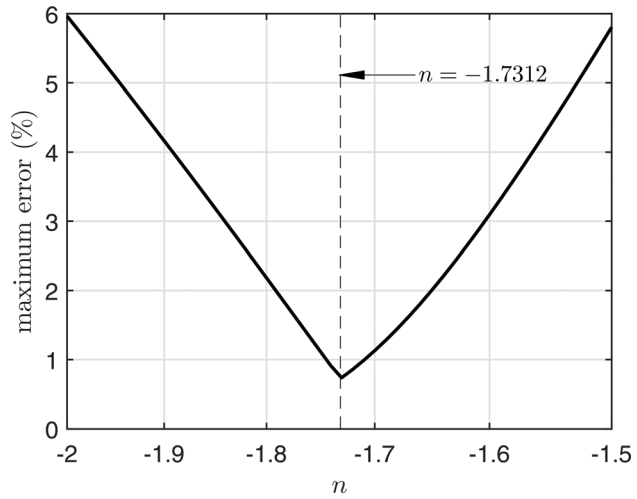

Fig. 5 Maximum blending error for isotherm width y_{max} as a function of blending parameter n

value of Ry. The correction factors tend to exactly a value of 1 (i.e., no correction needed) in their corresponding asymptotic regimes, and they cross over at $Ry_c = 0.7359$. Ry_c can be considered as a divider between Regime I and Regime II, with the understanding that in the vicinity of Ry_c the situation is actually intermediate between both regimes.

Choosing the right asymptotic expression, but neglecting the correction factors results in an error smaller than 10% for $Ry > 5.2611$ or $Ry < 0.1161$ in their corresponding regimes. As a heuristic easy to remember, omitting the correction factors results in an error inferior to 10% for $Ry > 20$ or $Ry < 0.05$.

Engineering expressions (with units) for the width of an isotherm for a point heat source on a semi-infinite solid can be obtained by replacing Eq. (13) into Eqs. (18) and (19), and combining with Eq. (10), obtaining

$$\hat{y}^{+}_{\max} = \hat{y}_{\max_{\mathrm{I}}} f_{y_{\max_{\mathrm{I}}}}(\mathrm{Ry}) = \sqrt{\frac{2}{\pi \mathrm{e}} \frac{\alpha q}{Uk(T_c - T_0)}} f_{y_{\max_{\mathrm{I}}}}(\mathrm{Ry}) \quad \text{for Regime I (fast)} \tag{21}$$

$$\hat{y}^{+}_{\max} = \hat{y}_{\max_{\mathrm{II}}} f_{y_{\max_{\mathrm{II}}}}(\mathrm{Ry}) = \frac{1}{2\pi} \frac{q}{k(T_c - T_0)} f_{y_{\max_{\mathrm{II}}}}(\mathrm{Ry}) \quad \text{for Regime II (slow)} \tag{22}$$

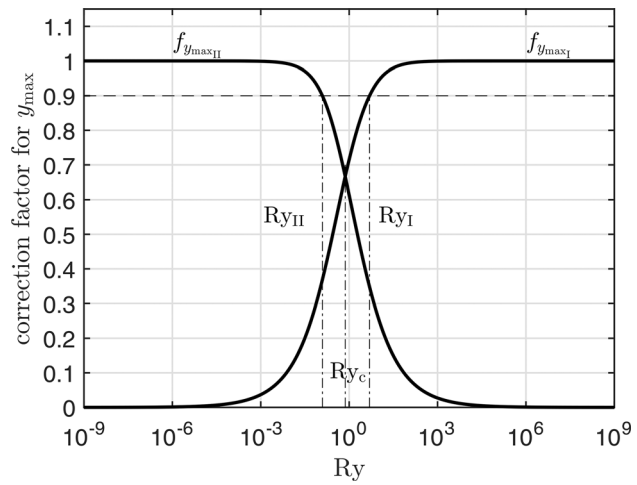

Fig. 6 Correction factors for maximum isotherm width y_{max}

Equations (21) and (22) are novel. Precursors of Eq. (21) (without the correction factor) were presented in Refs. [32] and [38]. Often, the combination q/U (with units of energy per unit length) is used as a parameter. For example, in the field of welding this combination is called "heat input" and is considered an essential variable by most codes and standards; because most welding procedures are performed in Regime I, the choice of using heat input makes practical sense, capturing the independent effects of heat source and travel velocity in a single easy-to-measure parameter without loss of information. Equation (22) shows that at low Ry, it is the power absorbed from the heat source q that determines the weld width not the ratio q/U. The low Ry Regime II is typically overlooked in codes and standards [43], despite that many practical cases can correspond to the low Ry regime, for example, some manual implementations of gas tungsten arc welding.

5 Scaling Analysis of Location x_{max} of Maximum Isotherm Width

The magnitude $x_{\max}$ is the location of maximum width of the isotherm $T(x, y, z) = T_c$ corresponding to the plane $z = 0$, as illustrated in Fig. 2. The magnitude $x_{\max}$ also indicates the location of the temperature peak along the line determined by $y = y_{\max}$, $z = 0$. The dependence of the dimensionless expression $x^*_{\max}$ on Ry is illustrated in Fig. 7, which displays similar features to Fig. 3.

Asymptotic analysis of Eq. (7), detailed in the Appendix, yields the following power laws:

$$\hat{x}^*_{\max_{\mathrm{I}}}(\mathrm{Ry}) = -\frac{\mathrm{Ry}}{\mathrm{e}} \quad \text{for Regime I (fast)} \tag{23}$$

$$\hat{x}^*_{\max_{\mathrm{II}}}(\mathrm{Ry}) = -\mathrm{Ry}^2 \quad \text{for Regime II (slow)} \tag{24}$$

The blending expression for $\hat{x}^{+}_{\max}(\mathrm{Ry})$ is obtained with the same process used to obtain $\hat{y}^{+}_{\max}(\mathrm{Ry})$, yielding the following correction factors:

$$f_{x_{\max_{\mathrm{I,II}}}}(\mathrm{Ry}) = [1 + (\mathrm{eRy})^{\pm n}]^{1/n} \tag{25}$$

where the exponent $+n$ corresponds to Regime I, and $-n$ corresponds to Regime II. The value of n for Eq. (25) was determined using the nested optimizations as it was done for $y_{\max}$. Figure 8 illustrates the blending error as a function of Ry for different values of n around the optimal, and Fig. 9 illustrates the variation of maximum error with blending parameter n. The minimax error is 1.9051%, corresponding to $n = -0.9990$.

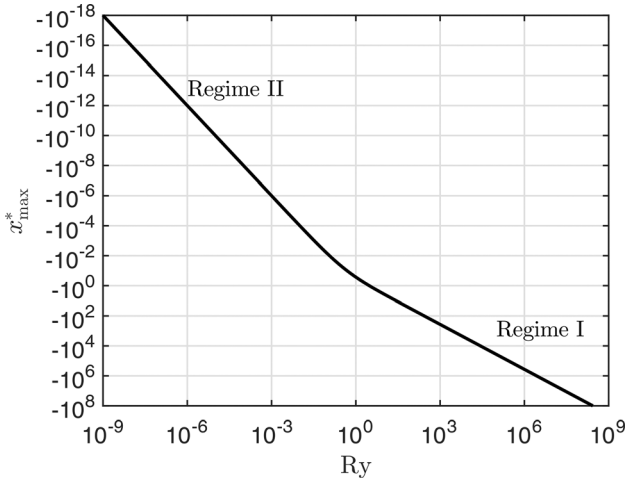

Fig. 7 Dimensionless location x_{max} of maximum isotherm width as a function of Ry

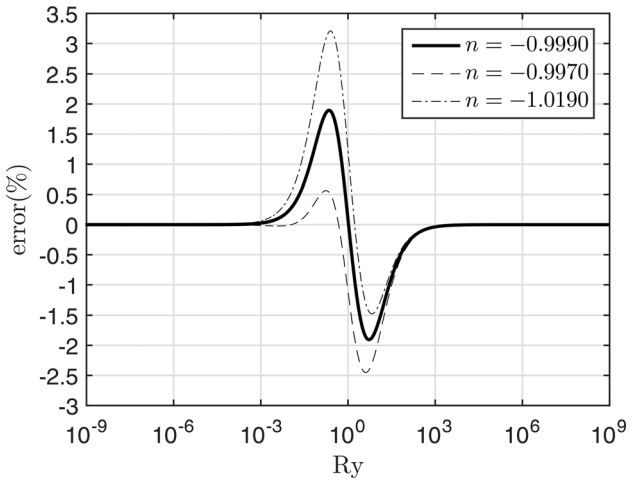

Fig. 8 Error of blending for location x_{max} of maximum isotherm width as a function of Ry for blending parameter n at or near the optimal value

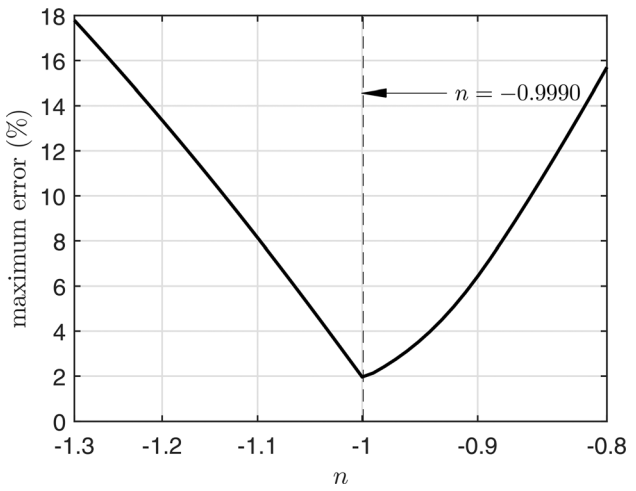

Fig. 9 Maximum blending error for location x_{max} of maximum isotherm width as a function of blending parameter n

The correction factors of Eq. (25) for the optimum value of $n = -0.9990$ are illustrated in Fig. 10 and have a similar power-law behavior in asymptotic regimes as seen Fig. 6. The crossover point for the correction factors in Fig. 10 is $\mathrm{Ry}_c = 0.3680$. Asymptotic expressions without correction factors result in an error smaller than 10% for $\mathrm{Ry_I} > 2.9829$ or $\mathrm{Ry_{II}} < 0.03543$ in their corresponding regimes. The same rule of thumb stated before also applies in this case: for $\mathrm{Ry} > 20$ or $\mathrm{Ry} < 0.05$, the asymptotic expressions alone result in predictions with an accuracy within 10% of the exact solution.

Expressions with units for the location of maximum isotherm width for a point heat source on a semi-infinite solid can be obtained by replacing Eq. (13) into Eqs. (23) and (24), and combining with Eq. (9) to obtain

$$\hat{x}^+_{\max} = \hat{x}_{\max_{\mathrm{I}}} f_{x_{\max_{\mathrm{I}}}}(\mathrm{Ry}) = -\frac{q}{2\pi e k(T_c - T_0)} f_{x_{\max_{\mathrm{I}}}}(\mathrm{Ry}) \quad \text{for Regime I (fast)} \tag{26}$$

$$\hat{x}^+_{\max} = \hat{x}_{\max_{\mathrm{II}}} f_{x_{\max_{\mathrm{II}}}}(\mathrm{Ry}) = -\frac{2U}{\alpha}\left[\frac{q}{4\pi k(T_c - T_0)}\right]^2 f_{x_{\max_{\mathrm{II}}}}(\mathrm{Ry}) \quad \text{for Regime II (slow)} \tag{27}$$

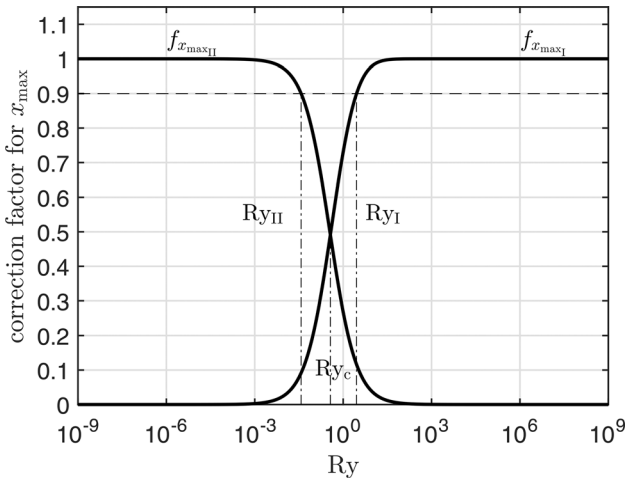

Fig. 10 Correction factors for location x_{max} of maximum isotherm width

For both asymptotic regimes, $x_{\max}$ and $y_{\max}$ have a parabolic relationship as follows:

$$\hat{y}_{\max_{\mathrm{I}}} = \sqrt{-\frac{4\alpha\hat{x}_{\max_{\mathrm{I}}}}{U}} \quad \text{for Regime I (fast)} \tag{28}$$

$$\hat{y}_{\max_{\mathrm{II}}} = \sqrt{-\frac{2\alpha\hat{x}_{\max_{\mathrm{II}}}}{U}} \quad \text{for Regime II (slow)} \tag{29}$$

with the following dimensionless counterparts:

$$\hat{y}^*_{\max_{\mathrm{I}}} = \sqrt{-2\hat{x}^*_{\max_{\mathrm{I}}}} \quad \text{for Regime I (fast)} \tag{30}$$

$$\hat{y}^*_{\max_{\mathrm{II}}} = \sqrt{-\hat{x}^*_{\max_{\mathrm{II}}}} \quad \text{for Regime II (slow)} \tag{31}$$

Equations (28) and (29) have the same functional dependence and very close magnitude to the thickness of a thermal boundary layer in low Prandtl number fluids, which is consistent with the parabolic Eulerian form of the governing differential equations.

6 Example of Application

The accuracy of the point heat source model used here was already assessed in Ref. [32] for the case of welding. In this section, the emphasis is on the mechanics of the use of the expressions developed in this paper.

Consider the welding of a 19-mm-thick plate of A36 steel using submerged arc welding with the following parameters: welding current of 600 A, voltage of 35 V, a travel speed of 12.7 mm/s, and no preheat ($T_0 = 20\,^\circ\mathrm{C}$). Representative properties for A36 steel are $k = 50$ W/mK and $\alpha = 1.4 \times 10^{-5}$ m^2/s. A representative process efficiency for submerged arc welding is $\eta = 0.99$ [38], resulting in a heat source of 21 kW, of which 20.79 kW are absorbed by the solid. The width of the weld bead is given by the width of the isotherm corresponding to the melting temperature (approximately 1460 °C for A36 steel)

$$\text{weld width} = 2y_{\max} \approx 2\hat{y}^+_{\max_{\mathrm{I}}} = 2\hat{y}_{\max_{\mathrm{I}}} f_{y_{\max_{\mathrm{I}}}}(\mathrm{Ry}) \tag{32}$$

For the conditions considered, the Rykalin number is $\mathrm{Ry} = 20.84$ (Eq. (13)), corresponding to Regime I (fast moving heat source, Fig. 6). Equation (21) yields $\hat{y}_{\max_{\mathrm{I}}} = 8.634$ mm, and Eq. (20) yields $f_{y_{\max_{\mathrm{I}}}} = 0.9694$. Consistent with the practical heuristic discussed earlier, for $\mathrm{Ry} > 20$, the error in omitting the correction factor is less than 10%. Replacing the calculated values

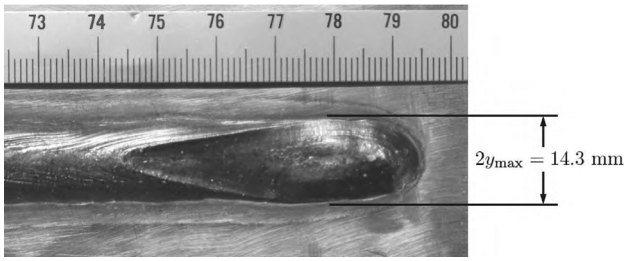

Fig. 11 Weld bead corresponding to Ry = 20.84. Scale is in mm.

into Eq. (32): $\hat{y}^+_{max_I} = 8.370$ mm, resulting in an estimated weld width of 16.74 mm.

A weld in the conditions considered was performed, and the power was stopped before reaching the end of the plate. The solidified weld bead is shown in Fig. 11 and displays the elongated shape expected from a high Rykalin number, with a measured width of 14.3 mm, indicating a relative error of the estimation of 17%. Considering that repeatability of width and depth measurements in welding is of the order of 10% and that tabulated thermophysical properties also involve significant uncertainty, an error of 17% between measurement and prediction is remarkable.

If this problem was approached using the asymptotic expressions of Regime II, the uncorrected estimation of Eq. (22) yields the unrealistic value of $\hat{y}_{max_{II}} = 45.96$ mm. Because the target parameters are far from the asymptotic regime considered, a correction factor is necessary. In this case, the correction factor is $f_{y_{max_{II}}} = 0.1821$, yielding almost exactly the same estimate as before: $\hat{y}^+_{max_{II}} = 8.369$ mm, and an estimated weld width of 16.74 mm.

7 Discussion

The analysis presented here dispels old misconceptions and brings new insights. The first misconception relates to normalization of Rosenthal's solution (Eq. (6)). The number of dimensionless groups related to this equation is four, not five as stated in Christensen's analysis [32], and there is no variable-free independent dimensionless group. Christensen's θ parameter required the unnecessary introduction of melting temperature in the set of parameters.

A second rectified misconception, embodied in most codes and standards for welding, is that heat input (q/U) is an essential parameter governing the behavior of the solution for a given material. This statement is true for Regime I (fast welds), but it is not true for slow welds, where the essential parameter is power of the heat source (q). For the case of welding, a survey of typical welding parameters [44] shows that most arc welding procedures have $Ry > 1$; however, some process and material combinations belong to Regime II ($Ry < 1$), for example, gas tungsten arc welding in steel and aluminum, gas metal arc welding in aluminum, and friction stir welding of aluminum. When $Ry < 1$, two welds with the same heat input do not necessarily have similar width.

Among the new insights is a rigorous understanding of the origins of the Rykalin number and its use to obtain quantitative results. In agreement with Ref. [45], this work suggests that the Rykalin number can be singled out as a key magnitude to characterize the behavior of a moving heat source in a thick substrate, in a way analogous to how the Reynolds number (Re) is essential to characterize fluid mechanics problems. There is an important conceptual difference between Re and Ry. For many types of flow, Re depends only on problem parameters: an externally imposed velocity, a characteristic length, and the kinematic viscosity of the fluid. On the other hand, Ry depends on the reference temperature chosen, and the same system can have different Ry assigned depending on the temperature of interest; for example, whether the melting temperature or solid-state phase transformations are the focus of interest.

Another insight presented for the first time is the application of Churchill–Usagi blending to moving heat sources. Blending enabled the construction of correction factors to account for deviations from the asymptotic regime. Two aspects of these correction factors were unexpected. First, that the correction factors result in accurate corrections even very far from the asymptotic regime, i.e., the correction factors do not "break down" outside their intended regime. Empirical correction factors, so common in heat transfer and many other engineering disciplines, very often are invalid far from the asymptotic regime. The second unexpected finding about the correction factors proposed is the very small error resulting from blending approximations, always below 2%.

The ultimate goal of the estimates and correction factors presented here is to serve as accurate predictors of actual processes, in a similar way that moving heat source equations from Ref. [46] are used in Ref. [28]. In these references, the asymptotic solutions are modified with empirical correction factors. These empirical modifications are not based on fundamental analysis, resulting in two important drawbacks: first, these modifications are valid only for the materials and processes used in the calibrations, and second, the range of parameters for which these calibrations are valid is not clearly defined.

The formulae proposed here can still differ from reality significantly, because the starting point is the Rosenthal model, which does not consider secondary (but non-negligible) effects such as finite thickness of substrate, finite size of heat source, variable materials properties, latent heat of phase change, and the effect of convection in the molten substrate material. The accuracy of predictions can be enhanced with additional correction factors, which are the focus of current efforts. In addition to corrections based on the balance between conduction and advection (captured by Ry), practical expressions must also account for other important factors not captured in Rosenthal's analysis. A methodology for blending through multiple dimensionless groups is currently inexistent and is also the focus of current efforts.

8 Conclusions

This work presents new practical and rigorous expressions for calculating the width of an isotherm (y_{max}, Eqs. (21) and (22)) and its location x_{max} along the x-axis (Eqs. (26) and (27)). The dimensionless form of these two magnitudes depends only on the Rykalin number, Ry, which is a metric of how fast or slow a heat source is. The Rykalin number divides all possible solutions in two regimes: Regime I corresponding to high Ry ("fast" heat sources) and low Ry ("slow" heat sources). Because Ry depends on a chosen temperature, moving heat sources cannot be deemed as intrinsically fast or slow until a temperature of interest is selected. The expressions proposed have the form of an asymptotic expression multiplied by a correction factor (Eq. (20) for y_{max}, and Eq. (25) for x_{max}). These expressions coincide with the exact solution in the asymptotic extremes, and the maximum error anywhere in the domain is 0.7326% for y_{max} and 1.9051% for x_{max}. For $Ry < 20$ or $Ry > 0.05$, the asymptotic expressions alone, without correction, have an error below 10%. The practical expressions presented here require much smaller computational effort than numerical methods, do not present convergence issues, and can be calculated using a handheld calculator or a basic spreadsheet; these expressions can also be used to estimate, for example, the width of a weld, the size of zone affected by the heat source in a number of processes, or to verify numerical models. The use of blending techniques is applied for the first time to the study of moving heat sources, and the results obtained support the applicability of asymptotics and blending techniques to tackle moving heat source problems.

Funding Data

- Student scholarship from the American Welding Society Alberta Section.

- Canadian Welding Association Foundation (CWA Foundation Post).
- China Scholarship Council.
- Natural Sciences and Engineering Research Council of Canada (Grant Nos. CRDPJ 462535-13 and RGPIN-2014-04892).

Appendix: Derivation of Asymptotic Behaviors

A surface isotherm is the curve $y^* = y^*(x^*)$ defined by the implicit equation $T^*(x^*, y^*, 0) = T_c^*$. The maximum width of this isotherm $y_{\max}^*$ and its location $x_{\max}^*$ define the point $\mathbf{x}_{\max}^* = (x_{\max}^*, y_{\max}^*, 0)$ on the surface. The location of $x_{\max}^*$ is given by the condition $dy^*/dx^*|_{T^*=T_c^*, z^*=0} = 0$, plus a negative second derivative condition which is fulfilled. This condition for the maximum can also be stated as $(\partial T^*/\partial x^*)/(\partial T^*/\partial y^*)|_{\mathbf{x}_{\max}^*} = 0$, which implies $\partial T^*/\partial x^*|_{\mathbf{x}_{\max}^*}$ when the denominator is not zero, which is also fulfilled. Using Eq. (7), the expression of this last derivative is

$$\frac{\partial T^*}{\partial x^*} = -\frac{\exp(-r^* - x^*)}{r^*}\left(\frac{x^*}{r^{*2}} + \frac{x^*}{r^*} + 1\right) \tag{A1}$$

At point $\mathbf{x}_{\max}^*$, the condition $\partial T^*/\partial x^* = 0$ implies

$$\frac{x_{\max}^*}{r_{\max}^{*2}} + \frac{x_{\max}^*}{r_{\max}^*} + 1 = 0 \tag{A2}$$

Also at point $\mathbf{x}_{\max}^*$, and keeping in mind that $\mathrm{Ry} = 1/T_c^*$, Eq. (7) can be rewritten as

$$\mathrm{Ry} = r_{\max}^* \exp(r_{\max}^* + x_{\max}^*) \tag{A3}$$

Regime I: Ry $\to \infty$. Replacing the definition of r (Eq. (2)) into Eq. (A3) yields

$$\mathrm{Ry} \to -x_{\max_\mathrm{I}}^* \sqrt{1 + \frac{y_{\max_\mathrm{I}}^{*2}}{x_{\max_\mathrm{I}}^{*2}}} \exp\left(x_{\max_\mathrm{I}}^* - x_{\max_\mathrm{I}}^* \sqrt{1 + \frac{y_{\max_\mathrm{I}}^{*2}}{x_{\max_\mathrm{I}}^{*2}}}\right) \tag{A4}$$

In Regime I, point $\mathbf{x}_{\max_\mathrm{I}}^*$ trails far behind the heat source, thus $r_{\max_\mathrm{I}}^* \to \infty$. In this situation, Eq. (A2) indicates that $r_{\max_\mathrm{I}}^* \to -x_{\max_\mathrm{I}}^*$, and the definition of r indicates that

$$x_{\max_\mathrm{I}}^* \to -\frac{1}{2} y_{\max_\mathrm{I}}^{*2} \tag{A5}$$

Considering that when $\varepsilon \to 0$, $\sqrt{1+\varepsilon} \to 1 + \frac{1}{2}\varepsilon$, Eq. (A4) becomes

$$\mathrm{Ry} \to -x_{\max_\mathrm{I}}^* \left(1 + \frac{1}{x_{\max_\mathrm{I}}^*}\right) \exp\left[-x_{\max_\mathrm{I}}^* - x_{\max_\mathrm{I}}^* \left(1 + \frac{1}{x_{\max_\mathrm{I}}^*}\right)\right] \tag{A6}$$

resulting in

$$\mathrm{Ry} \to -\mathrm{e} x_{\max_\mathrm{I}}^* \tag{A7}$$

Equations (A5) and (A7) yield Eqs. (23) and (18).

Regime II: Ry $\to$ 0. Equation (A3) indicates that when $\mathrm{Ry} \to 0$, $r_{\max_\mathrm{II}}^* \to 0$. Also, Eq. (A2) indicates that in this condition $x_{\max_\mathrm{II}}^* \to -r_{\max_\mathrm{II}}^{*2}$. Replacing these trends in a dimensionless form of Eq. (2), and keeping in mind that $x_{\max_\mathrm{II}}^{*2}$ tends to zero faster than $x_{\max_\mathrm{II}}^*$, we obtain

$$x_{\max_\mathrm{II}}^* \to -y_{\max_\mathrm{II}}^{*2} \tag{A8}$$

In Regime II, when $r_{\max_\mathrm{II}}^* \to 0$, $x_{\max_\mathrm{II}}^* \to 0$ and the exponential in Eq. (A3) then tends to 1. Replacing Eq. (A8) in a dimensionless form of Eq. (2), and keeping in mind that $y_{\max_\mathrm{II}}^{*4}$ tends to zero faster than $y_{\max_\mathrm{II}}^{*2}$, we obtain

$$\mathrm{Ry} \to y_{\max_\mathrm{II}}^* \tag{A9}$$

Equations (A8) and (A9) yield Eqs. (24) and (19).

References

[1] Rosenthal, D., 1935, "Etude Théorique Du Régime Thermique Pendant La Soudure à L'Arc," Comptes Rendus (2eme Congres National Des Sciences), pp. 1277–1292.
[2] Rosenthal, D., 1946, "The Theory of Moving Sources of Heat and Its Application to Metal Treatments," Trans. ASME, **68**, pp. 849–866.
[3] Rykalin, N. N., 1951, *Calculation of Heat Flow in Welding*, Mashgis, Moscow, Russia.
[4] Li, W. B., Easterling, K. E., and Ashby, M. F., 1986, "Laser Transformation Hardening of Steel-II. Hypereutectoid Steels," Acta Metall., **34**(8), pp. 1533–1543.
[5] Komanduri, R., and Hou, Z. B., 2001, "Thermal Analysis of the Laser Surface Transformation Hardening Process," Int. J. Heat Mass Transfer, **44**(15), pp. 2845–2862.
[6] Hill, J. W., Lee, M. J., and Spalding, I. J., 1974, "Surface Treatments by Laser," Opt. Laser Technol., **6**(6), pp. 276–278.
[7] Hou, Z. B., and Komanduri, R., 2000, "General Solutions for Stationary/Moving Plane Heat Source Problems in Manufacturing and Tribology," Int. J. Heat Mass Transfer, **43**(10), pp. 1679–1698.
[8] Jaeger, J. C., 1942, "Moving Sources of Heat and the Temperature of Sliding Contacts," Proc. R. Soc. New South Wales, **76**, pp. 203–224.
[9] Bulsara, V. H., Ahn, Y., Chandrasekar, S., and Farris, T. N., 1997, "Polishing and Lapping Temperatures," ASME J. Tribol., **119**(1), pp. 163–170.
[10] Malkin, S., 1974, "Thermal Aspects of Grinding: Part 2 – Surface Temperatures and Workpiece Burn," ASME J. Eng. Ind., **96**(4), pp. 1184–1191.
[11] Komanduri, R., and Hou, Z. B., 2009, "Unified Approach and Interactive Program for Thermal Analysis of Various Manufacturing Processes With Application to Machining," Mach. Sci. Technol., **13**(2), pp. 143–176.
[12] Dutt, R. P., and Brewer, R. C., 1965, "On the Theoretical Determination of the Temperature Field in Orthogonal Machining," Int. J. Prod. Res., **4**(2), pp. 91–114.
[13] Kolonits, F., 2016, "Analysis of the Temperature of the Rail/Wheel Contact Surface Using a Half-Space Model and a Moving Heat Source," Proc. Inst. Mech. Eng., Part F, **230**(2), pp. 502–509.
[14] Knothe, K., and Liebelt, S., 1995, "Determination of Temperatures for Sliding Contact With Applications for Wheel-Rail Systems," Wear, **189**(1–2), pp. 91–99.
[15] Wei, P. S., and Giedt, W. H., 1985, "Surface Tension Gradient-Driven Flow Around an Electron Beam Welding Cavity," Weld. J., **64**(9), pp. s251–s259.
[16] Friedman, E., 1975, "Thermomechanical Analysis of the Welding Process Using the Finite Element Method," ASME J. Pressure Vessel Technol., **97**(3), pp. 206–213.
[17] Goldak, J., Chakravarti, A., and Bibby, M., 1984, "A New Finite Element Model for Welding Heat Sources," Metall. Trans. B, **15**(2), pp. 299–305.
[18] Rohsenow, W. M., Hartnett, J. P., and Cho, Y. I., 1998, *Handbook of Heat Transfer*, 3rd ed., McGraw-Hill, New York.
[19] Eagar, T. W., and Tsai, N. S., 1983, "Temperature Fields Produced by Traveling Distributed Heat Sources," Weld. J., **62**(12), pp. 346–355.
[20] Van Elsen, M., Baelmans, M., Mercelis, P., and Kruth, J.-P., 2007, "Solutions for Modelling Moving Heat Sources in a Semi-Infinite Medium and Applications to Laser Material Processing," Int. J. Heat Mass Transfer, **50**(23–24), pp. 4872–4882.
[21] Winczek, J., 2010, "Analytical Solution to Transient Temperature Field in a Half-Infinite Body Caused by Moving Volumetric Heat Source," Int. J. Heat Mass Transfer, **53**(25–26), pp. 5774–5781.
[22] Gajapathi, S. S., Mitra, S. K., and Mendez, P. F., 2011, "Controlling Heat Transfer in Micro Electron Beam Welding Using Volumetric Heating," Int. J. Heat Mass Transfer, **54**(25–26), pp. 5545–5553.
[23] Mendez, P. F., Tello, K. E., and Gajapathi, S. S., 2012, "Generalization and Communication of Welding Simulations and Experiments Using Scaling Analysis," Ninth International Conference on Trends in Welding Research, Chicago, IL, June 4–8, pp. 249–258.
[24] Mendez, P. F., 2011, "Synthesis and Generalisation of Welding Fundamentals to Design New Welding Technologies: Status, Challenges and a Promising Approach," Sci. Technol. Weld. Joining, **16**(4), pp. 348–356.
[25] Muzychka, Y. S., and Yovanovich, M. M., 2001, "Thermal Resistance Models for Non-Circular Moving Heat Sources on a Half Space," ASME J. Heat Transfer, **123**(4), pp. 624–632.
[26] Incropera, F. P., and DeWitt, D. P., 1985, *Fundamentals of Heat and Mass Transfer*, 2nd ed., Wiley, New York.
[27] Özisik, M. N., 1993, *Heat Conduction*, 2nd ed., Wiley, New York.
[28] Seyffarth, P., Meyer, B., and Scharff, A., 1992, *Grosser Atlas Schweiss-ZTU-Schaubilder*, Fachbuchreihe Schweisstechnik. Deutscher Verlag für Schweisstechnik, Düsseldorf, Germany.

[29] Wood, G., Islam, S. A., and Mendez, P. F., 2014, "Calibrated Expressions for Welding and Their Application to Isotherm Width in a Thick Plate," Soldagem Inspeção, **19**(3), pp. 212–220.
[30] Wilson, H. A., 1904, "On Convection of Heat," Proc. Cambridge Philos. Soc., **12**, pp. 406–423.
[31] Roberts, O. F. T., 1923, "The Theoretical Scattering of Smoke in a Turbulent Atmosphere," Proc. R. Soc. A, **104**(728), pp. 640–654.
[32] Christensen, N., Davies, V., de, L., and Gjermundsen, K., 1965, "Distribution of Temperatures in Arc Welding," British Weld. J., **12**(2), pp. 54–75.
[33] Mendez, P. F., 2010, "Characteristic Values in the Scaling of Differential Equations in Engineering," ASME J. Appl. Mech., **77**(6), p. 061017.
[34] Dantzig, J. A., and Tucker, C. L., 2001, *Modeling in Materials Processing*, Cambridge University Press, Cambridge, UK.
[35] Buckingham, E., 1914, "On Physically Similar Systems; Illustrations of the Use of Dimensional Equations," Phys. Rev., **4**(4), pp. 345–376.
[36] Washio, T., and Motoda, H., 1999, "Extension of Dimensional Analysis for Scale-Types and Its Application to Discovery of Admissible Models of Complex Processes," International Workshop on Similarity Method, pp. 129–147.
[37] Myhr, O. R., and Grong, Ø., 1990, "Dimensionless Maps for Heat Flow Analyses in Fusion Welding," Acta Metall. Et Mater., **38**(3), pp. 449–460.
[38] Grong, Ø., 1994, *Metallurgical Modelling of Welding*, 1st ed., Institute of Materials, Cambridge, UK.
[39] Fuerschbach, P. W., and Eisler, G. R., 2002, "Determination of Material Properties for Welding Models by Means of Arc Weld Experiments," Sixth International Trends in Welding Research, Pine Mountain, Georgia, Apr. 15–19.
[40] Churchill, S. W., and Usagi, R., 1972, "A General Expression for the Correlation of Rates of Transfer and Other Phenomena," AIChE J., **18**(6), pp. 1121–1128.
[41] Mendez, P. F., and Eagar, T. W., 2012, "Order of Magnitude Scaling: A Systematic Approach to Approximation and Asymptotic Scaling of Equations in Engineering," ASME J. Appl. Mech., **80**(1), p. 011009.
[42] Mendez, P. F., and Ordóñez, F., 2005, "Scaling Laws From Statistical Data and Dimensional Analysis," ASME J. Appl. Mech., **72**(5), pp. 648–657.
[43] Goldak, J., Asadi, M., and Alena, R. G., 2010, "Why Power Per Unit Length of Weld Does Not Characterize a Weld?," Comput. Mater. Sci., **48**(2), pp. 390–401.
[44] The James F. Lincoln Arc Welding Foundation, 2000, *The Procedure Handbook of Arc Welding*, 14th ed., The James F. Lincoln Arc Welding Foundation, Cleveland, OH.
[45] Fuerschbach, P. W., 1995, "A Dimensionless Parameter Model for Arc Welding Processes," Fourth International Conference on Trends in Welding Research, Gatlinburg, TN, June 5–8, pp. 493–497.
[46] Inagaki, M., Nakamura, H., and Okada, A., 1965, "Studies of Cooling Processes in the Cases of Welding With Coated Electrode and Submerged Arc Welding," J. Jpn. Weld. Soc., **34**(10), pp. 1064–1075.